

Comparative validation of the radar interferometry-based SYM12 Using ICESat-2 ATL03 and ground-based GPS measurements

Yunus Kaya*¹ 

¹ Harran University, Faculty of Engineering, Department of Geomatics Engineering, Şanlıurfa, Türkiye; yunuskaya@harran.edu.tr



Article History:

Received: 25 March 2025

Revised: 18 April 2025

Accepted: 24 April 2025

Published: 30 June 2025



Copyright: © 2025 by the authors.

This article is an open access article distributed under terms and conditions of the Creative Commons Attribution (CC BY-SA) license. <https://creativecommons.org/licenses/by-sa/4.0/>

Abstract: This study evaluates the performance of the SYM12 digital surface model, derived from radar interferometry between 2011 and 2014, by comparing it with two reference datasets: the ICESat-2 ATL03 lidar altimeter (2018–2023) and 879 GPS ground control points measured in 2024. Relationships between SYM12, ICESat-2 ATL03, and GPS measurements were tested using root mean square error (RMSE), mean absolute error (MAE), and Pearson correlation coefficient analysis. Both unfiltered and interquartile range (IQR) filtered data were analyzed. Results indicate a strong correlation ($R > 0.99$) between SYM12, ICESat-2 ATL03, and GPS observations in low- and mid-elevation regions, while discrepancies increase in high-elevation and complex terrain areas. Filtering improved the performance of SYM12 relative to ATL03, reducing the RMSE from 35.54 m to 2.24 m and the MAE from 5.10 m to 1.60 m. Notably, RMSE and MAE values remained higher in high-altitude areas. For SYM12-GPS comparisons, the RMSE and MAE were 2.32 m and 1.56 m, respectively, while GPS-ATL03 comparisons yielded RMSE and MAE values of 0.60 m and 0.39 m, respectively. This study underscores the value of integrating newer lidar-based datasets, such as ATL03, to enhance the accuracy of DSMs derived from radar interferometry.

Keywords: Digital surface model (DSM12); ICESat-2 ATL03; radar interferometry; lidar altimetry

Citation: Kaya, Y. (2025). Comparative validation of the radar interferometry-based SYM12 Using ICESat-2 ATL03 and ground-based GPS measurements. *Turk. J. Remote Sens.*, 7(1), 53-68. <https://doi.org/10.51489/tuzal.1665238>

1. Introduction

Digital Surface Models (DSMs) have become an indispensable tool in modern science, engineering, and environmental analysis (Dibs et al., 2023). Representing the Earth's surface and capturing both natural and man-made features, these models are an integral component of various applications such as urban planning, disaster management, hydrological modeling, and terrain analysis (Van Westen, 2013; Sahani et al., 2019; Guo et al., 2021; Oksanen & Sarjakoski, 2005; Gazioğlu et al., 2014; Kılıç et al., 2022). Global DSMs are distributed at varying resolutions and are often available free of charge (Mesa-Mingorance & Ariza-López, 2020). These global DSMs are typically used as base data for studies that do not require high spatial resolution. However, their resolution is insufficient for applications that demand greater accuracy. This growing demand for precision in such fields underscores the need for high-resolution and highly accurate DSMs. With technological advancements, the role of DSMs in decision-making processes has increased exponentially, highlighting their critical importance in both global and regional geospatial studies (Quamar et al., 2023). The accuracy of DSMs is particularly vital for tasks requiring fine-scale detail, such as infrastructure development, floodplain mapping, and precision agriculture (Schumann et al., 2019; Anders et al., 2020). Users including government agencies, researchers, and private enterprises continuously seek reliable and up-to-date geospatial data to make informed decisions. This demand has driven the advancement of cutting-edge remote sensing technologies such as radar interferometry (Rosen et al., 2000), LiDAR (Ulvi & Yiğit, 2022; Yiğit et al., 2023), and

satellite-based Earth observation systems (Loew et al., 2017), among others (Panda et al., 2016; Joshi et al., 2016).

In Turkey, the importance of high-quality Digital Surface Models (DSMs) has become increasingly prominent due to the country's diverse topography and growing infrastructure demands. From mountainous regions to vast plains and urbanized areas, high-accuracy surface models are essential for the planning and management of national projects (Moore et al., 1993). In response to Turkey's geographical and infrastructural requirements, the General Directorate of Mapping (HGM) has developed the SYM12 Digital Surface Model, a high-resolution dataset tailored to national needs. The data acquisition process spanned from 2011 to 2014 and covered the entire geographic extent of Turkey. Additionally, the dataset was refined according to Level-2 standards, incorporating corrections for gross errors and water surfaces, thereby enhancing its usability across a wide range of applications. Produced under the TanDEM-X High-Resolution Elevation Data Exchange Project (TReX), SYM12 utilizes radar interferometric data acquired from the TanDEM-X and TerraSAR-X satellites (Karataş & Yaman, 2024). Radar interferometry involves capturing radar signals from two satellite platforms and using the phase difference between the signals to construct elevation models. This methodology enables consistent and reliable surface modeling even in areas with dense vegetation or persistent cloud cover, where optical-based methods may face limitations. The SYM12 dataset features an approximate 12-meter spatial sampling interval, with a horizontal positional accuracy of ± 5 –10 meters and an absolute vertical accuracy of ± 4 meters, making it a valuable foundation for large-scale analyses. By integrating both natural and man-made features into a single dataset, SYM12 provides a comprehensive and precise representation of the Earth's surface. However, the ± 4 m absolute vertical accuracy may limit the applicability of SYM12 in highly sensitive or precision-critical projects.

The Ice, Cloud, and Land Elevation Satellite-2 (ICESat-2) represents a transformative advancement in satellite-based Earth observation, particularly in the measurement of surface elevations. Launched by NASA in 2018, ICESat-2 is equipped with the Advanced Topographic Laser Altimeter System (ATLAS), a state-of-the-art photon-counting lidar instrument that delivers exceptional precision in capturing surface elevation data. Among its primary data products, the ATL03 photon cloud dataset holds particular significance, providing geolocated photon returns with sub-meter accuracy in both horizontal and vertical dimensions. This level of precision makes ICESat-2 ATL03 data a valuable asset for evaluating the accuracy of surface models such as SYM12, which is based on remote sensing techniques like radar interferometry. ICESat-2 data were selected for DSM validation due to three key reasons. First, ICESat-2 offers significantly higher vertical accuracy compared to data derived from radar altimetry. Second, ICESat-2 observations are globally distributed and deliver consistent and reliable measurements across diverse terrain types, including challenging environments such as dense vegetation, urban areas, and water surfaces. Third, the photon-counting system employed by ICESat-2 generates a dense point cloud, enabling detailed surface characterization and the detection of subtle elevation changes. This allows for the classification of photon returns into land, water, ocean, sea ice, land ice, or inland water surfaces, thereby facilitating more effective terrain analysis.

Numerous studies in the literature have focused on leveraging ICESat-2 data to enhance the accuracy of global Digital Surface Models (DSMs) (Li et al., 2022a; Li et al., 2023; Li et al., 2024). Li et al. (2023) examined the accuracy of DSMs in regions covered by ICESat-2 and developed an attribute set to explore the sources of error in global DSMs. They applied a regression model to correct DSM elevations and found that LiDAR altimetry data could be effectively applied to more than 90% of the terrain. The improvements in the Shuttle Radar Topography Mission (SRTM) model ranged from 27.77% to 44.64% depending on the topographic type. In another study, Li et al. (2022a) utilized over 240,000 high-quality ATL08 photons to enhance the accuracy of three global DSMs. As a result, the Root Mean Square

Errors (RMSEs) of the Copernicus, NASA, and AW3D30 DSMs were reported as 6.73 m, 6.59 m, and 6.63 m, respectively. Furthermore, Li et al. (2024) applied ICESat-2 data to correct ASTER GDEM elevations, achieving RMSE improvements ranging from 16% to 82%, with an average improvement of 47%. In polar applications, Shen et al. (2022) utilized ICESat-2 data to identify ice sheets and ice shelves in Antarctica. Surface elevation estimates were derived at 500 m and 1 km resolutions based on DSMs constructed from ICESat-2 observations. Similarly, Li et al. (2022b) aimed to enhance the accuracy of the SRTM DSM in forested regions using ICESat-2 data. In their study, spatial interpolation methods based on ICESat-2 photons were applied, reducing the RMSE of the SRTM from 9.8 m to 4.2 m in the study area. While these studies provide comprehensive analyses on the improvement of global DSMs, there remains a gap in the literature concerning the refinement of locally produced DSMs. In particular, the accuracy of SYM12, developed by the General Directorate of Mapping (HGM) and serving as a foundational dataset for all of Turkey, has not been sufficiently investigated in the literature.

The primary objective of this study is to assess the vertical accuracy of the SYM12 dataset by comparing it with ICESat-2 data. Additionally, the study evaluates the accuracy of both datasets using ground-based GPS measurements that are spatially distributed in a homogeneous manner across the study area. To assess the vertical accuracy of SYM12 using ICESat-2 ATL03 data, it is necessary to co-register the two datasets and extract the corresponding SYM12 raster values at the locations of the ATL03 photon returns. The high spatial resolution and precision of the ATL03 dataset enable the evaluation of localized elevation discrepancies, while TG20 geoid corrections are applied to ensure that all comparisons are made within a consistent vertical reference framework. This methodology not only facilitates the assessment of SYM12's accuracy but also allows for the identification of potential systematic biases and the generation of regional error analyses within the DSM.

2. Materials and Methods

2.1. Study area

The study area is located in the southwestern region of Turkey, within the province of Isparta, and encompasses a landscape characterized by diverse topographic features such as mountainous terrain, flat plains, and forested regions (Figure 1). The area spans approximately 15 arc-minutes by 15 arc-minutes, situated between Lake Eğirdir and Lake Beyşehir. This region's geographical diversity and varying elevation levels make it an ideal test site for evaluating the accuracy of high-resolution Digital Surface Models (DSMs).

2.2. Materials

2.2.1. Digital surface model (SYM12)

The SYM12 Digital Surface Model is an elevation dataset produced as part of the TanDEM-X High-Resolution Elevation Data Exchange Project (TReX). Generated using radar interferometry techniques, SYM12 integrates data from the TanDEM-X and TerraSAR-X satellites to capture detailed topographic characteristics of the Earth's surface. This dataset incorporates both natural and anthropogenic features, including vegetation cover and man-made structures, providing a comprehensive representation of the terrain. SYM12 features a spatial sampling interval of 1/3 arc-second (approximately 12 meters), a horizontal positional accuracy of ± 5 –10 meters, and an absolute vertical accuracy of ± 4 meters. The dataset is structured in $1^\circ \times 1^\circ$ geographic tiles based on geographic coordinate grids, referenced to the WGS84 horizontal datum and the EGM-08 vertical datum. During its production between 2011 and 2014, the dataset underwent correction processes to mitigate gross errors and improve representation of water surfaces. It was refined to Level-2 standards, enhancing its usability across diverse applications. The SYM12-SAM12 product suite is specifically designed to ensure precision and reliability in projects that demand high

spatial accuracy. With its nationwide coverage and resolution, SYM12 serves as a critical tool in a variety of applications, including infrastructure planning, hydrological modeling, and regional geospatial analysis.

2.2.2. ICESat-2 ATL03

Launched in September 2018, ICESat-2 builds upon the legacy of the original ICESat mission (2003–2009), which pioneered the use of satellite-based laser altimetry (Schutz et al., 2005). Equipped with the Advanced Topographic Laser Altimeter System (ATLAS), ICESat-2 offers significant advantages in spatial and temporal resolution, enabling highly precise surface elevation measurements across diverse terrain types. Unlike its predecessor, ICESat-2 collects data continuously along 1,387 Reference Ground Tracks (RGTs) with a 91-day repeat cycle, providing comprehensive and consistent global coverage. Each RGT contains three beam pairs, with each pair consisting of a strong and weak beam (gt1l, gt1r, gt2l, gt2r, gt3l, gt3r) that are separated by 90 meters across-track, and spaced approximately 3 km along-track and 2.5 km across-track (Neumann et al., 2020). The ATL03 product, used in this study, consists of geolocated photon data with sub-meter accuracy in both horizontal and vertical dimensions. Each photon is georeferenced with parameters such as latitude, longitude, ellipsoidal height, confidence flags, and height corrections (Gao et al., 2023). These data enable detailed surface characterization, capturing fine-scale elevation variations and distinguishing between surface types such as land, water, and vegetation. In this study, ICESat-2 ATL03 data in .h5 format were used. The dataset was spatially constrained to match the coordinate extent of the raster-based surface model (Figure 1), and only photons within the study area boundary were utilized.

2.2.3. Türkiye geoid model (TG20)

The TG20 geoid model, developed by the General Directorate of Mapping (HGM), is the official geoid model used for Turkey and surrounding regions, covering the geographic extent of 35°N–43°N latitude and 25°E–45°E longitude (Simav et al., 2021). TG20 is a hybrid geoid model that integrates approximately 265,000 terrestrial gravity measurements, the global geopotential model GOCO06S, and the SRTM V4.1 digital elevation model at a resolution of 7.2 arc-seconds. The transformation of TG20 to Turkey's modern vertical reference system was achieved using a four-parameter transformation model, calibrated with data from 182 strategically distributed GPS/leveling stations across the country. To validate the model, 278 independent GPS/leveling stations were used, resulting in a standard deviation of less than 2 cm between the observed and predicted values (Yıldız et al., 2021). In this study, the TG20 model at a resolution of 1 arc-minute was used to convert ellipsoidal heights from the ICESat-2 ATL03 product into orthometric heights.

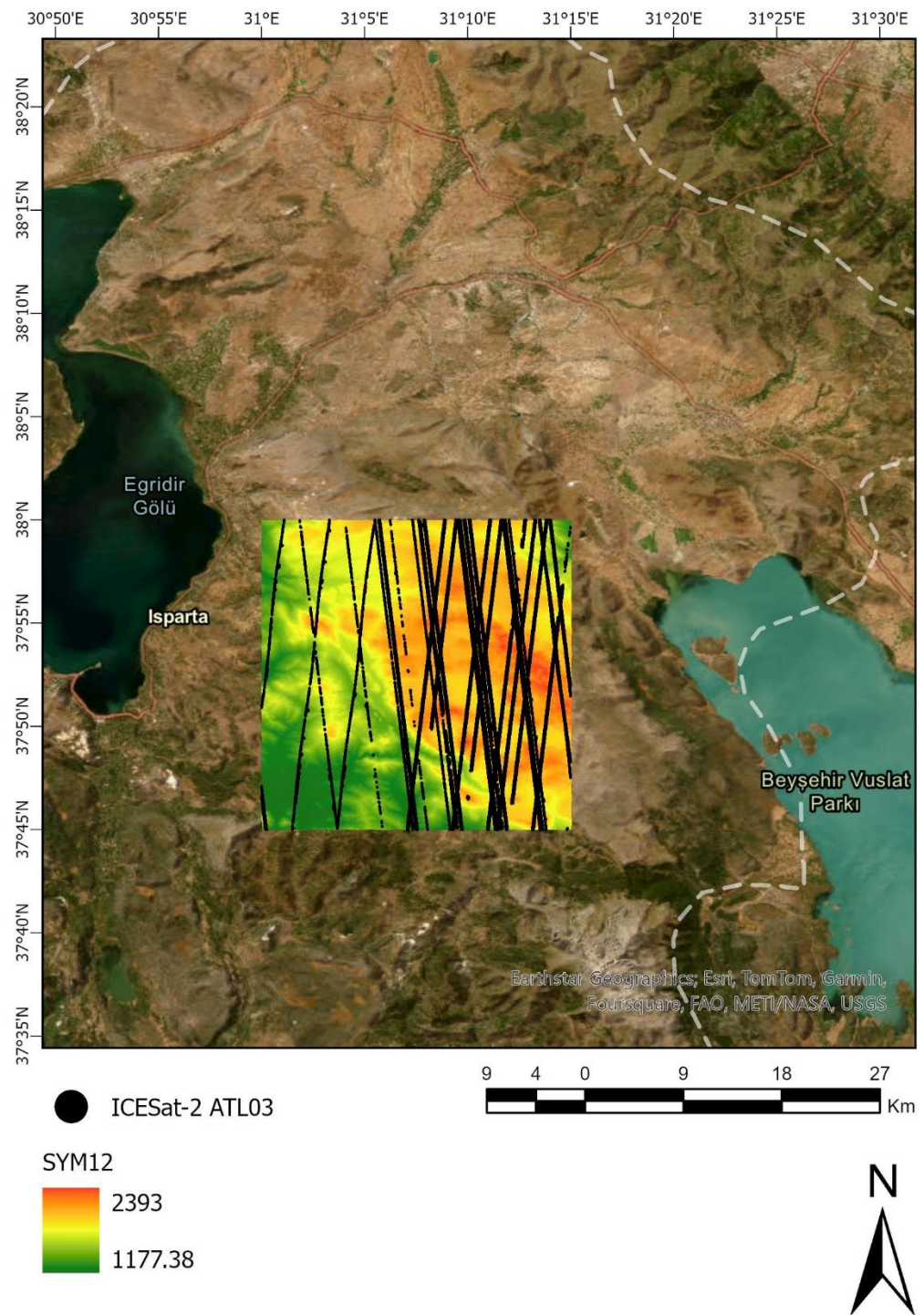


Figure 1. Study area

2.2.4. Validation data (GPS)

A total of 879 ground control points (GCPs) were measured using high-precision Global Positioning System (GPS) equipment, uniformly distributed throughout the study area. The selection of these points followed a strategic approach to ensure comprehensive coverage of diverse topographic and environmental conditions. Each measurement provided ellipsoidal heights relative to the WGS84 reference ellipsoid, which were subsequently converted to orthometric heights using the TG20 geoid model. This transformation ensured that height values derived from GPS were aligned with the vertical datum used for SYM12 and ICESat-2 ATL03, enabling direct and consistent vertical accuracy assessments across all datasets. The large number and spatial density of these control points enhanced the statistical robustness of the validation process, allowing for the detection of both local discrepancies and broader

systematic errors. Moreover, the inherent high accuracy of GPS observations provided a reliable benchmark against which the performance of remote sensing data could be rigorously evaluated, thereby reinforcing the overall validity of the study’s quantitative findings.

2.3. Methodology

The methodology of this study focuses on the comparative analysis of ICESat-2 ATL03 data and SYM12 surface model data. In addition, the reliability of both datasets was assessed using GPS measurements that are homogeneously distributed throughout the study area. An overview of the methodological workflow is presented in Figure 2.

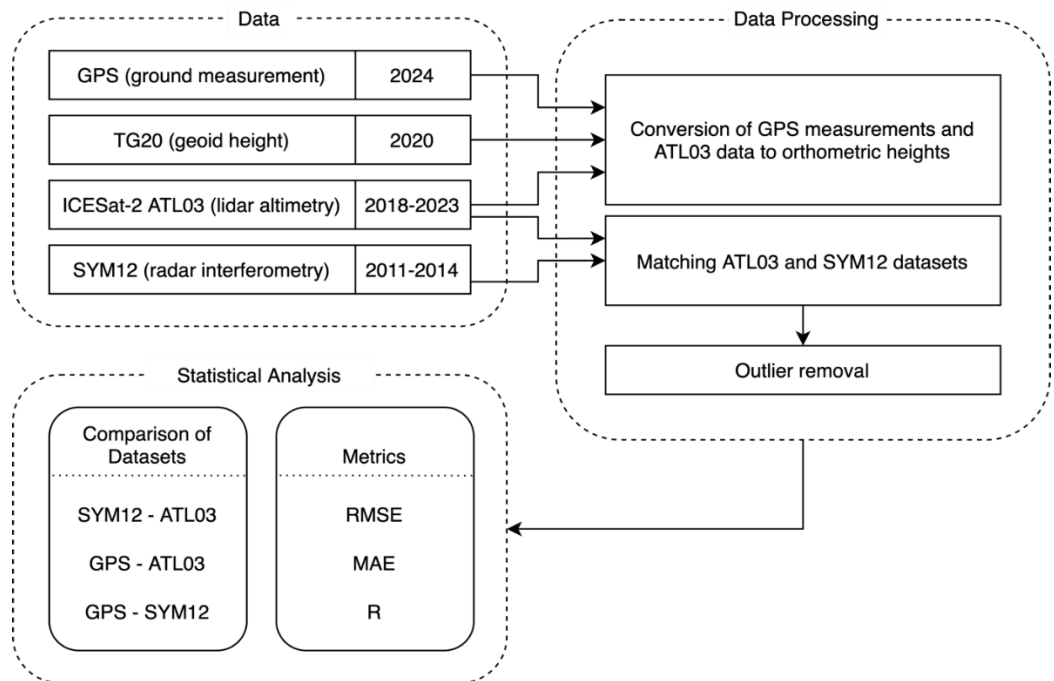


Figure 2. Workflow diagram

2.3.1. Download and preprocessing of ATL03 data

In this study, the ATL03 V006 dataset was acquired in HDF5 (.h5) format from the Distributed Active Archive Center (DAAC) of the National Snow and Ice Data Center (NSIDC). ATL03 provides geolocated photon data with sub-meter precision, offering detailed insights for surface elevation analysis. The dataset includes two essential parameters used to filter and identify the most reliable photons for the study: *quality_ph* (photon quality) and *signal_conf_ph* (photon signal confidence). The *quality_ph* parameter can assume four values: 0 (nominal), 1 (possible afterpulse), 2 (possible impulse response effect), and 3 (non-transmitter echo pulse, TEP). The *signal_conf_ph* parameter expresses the signal confidence of photons over five surface types—land, ocean, sea ice, land ice, and inland water—using a seven-level classification ranging from -2 to 4. Values of -2 and -1 represent photons unrelated to the target surface, while values 0 and 1 indicate noise. Values 2, 3, and 4 correspond to low, medium, and high signal confidence, respectively. In this study, only photons reflected from land surfaces with *quality_ph* = 0 and *signal_conf_ph* = 4 were selected, ensuring that the data used in the analysis were of the highest possible accuracy and reliability.

2.3.2. Integration of ATL03 and SYM12 data

The integration of SYM12 data with ICESat-2 ATL03 photon data was carried out to ensure precise spatial alignment and accurate comparison of elevation values. Each photon in the ATL03 dataset was geospatially matched to the nearest corresponding SYM12 grid cell,

allowing for the extraction of elevation values from the closest spatial point within the SYM12 raster. This spatial matching process was conducted within the WGS84 geographic coordinate system to maintain consistency between the datasets. For each ATL03 photon, the nearest SYM12 elevation value was determined based on horizontal proximity using a nearest neighbor interpolation approach. This method enabled the evaluation of elevation differences between the datasets at the most relevant and representative locations. To perform nearest neighbor interpolation based on geographic coordinates, it was first necessary to define an ellipsoidal distance function. For this purpose, the Haversine formula, a widely used method in the literature, was applied (Courellis et al., 2016). To implement the Haversine calculation, the latitude and longitude values from both datasets must be defined. Let $\{(\varphi_i, \lambda_i, z_i)\}_{i=1}^{N_{SYM12}}$ represent the set of SYM12 raster data points, where φ_i and λ_i are the latitude and longitude in radians, and z_i is the elevation at that coordinate. For each ATL03 photon located at coordinates (φ_p, λ_p) , the corresponding elevation value is denoted as $z_p = z_j$, where j is determined according to Equation (1).

$$j = \arg \min_{1 \leq i \leq N} d_{hav}((\varphi_p, \lambda_p), (\varphi_i, \lambda_i)) \tag{1}$$

where, d_{hav} denotes the Haversine distance function, which is calculated using Equation (2).

$$d_{hav}((\varphi_p, \lambda_p), (\varphi_i, \lambda_i)) = 2R \arcsin \left(\sqrt{\sin^2 \left(\frac{\varphi_p - \varphi_i}{2} \right) + \cos(\varphi_p) \cos(\varphi_i) \sin^2 \left(\frac{\lambda_p - \lambda_i}{2} \right)} \right) \tag{2}$$

where, R represents the mean radius of the Earth (approximately 6371 km); φ_p and φ_i denote the latitudes of the ATL03 photon and the i -th grid cell, respectively; λ_p and λ_i denote the corresponding longitudes; z_p is the elevation value assigned to the ATL03 photon, obtained from the nearest SYM12 grid cell.

The arg min operation returns the index i that minimizes the Haversine distance.

2.1.3. Elimination of outliers

To ensure the reliability of the elevation comparison between ICESat-2 ATL03 photons and the SYM12 surface model, a systematic outlier elimination procedure was implemented. Each ATL03 photon was first matched to the corresponding SYM12 elevation value using a nearest neighbor distance approach, allowing vertical differences between the photon data and the model to be represented at the closest spatial point. Following this, the absolute vertical differences between the matched data points were calculated in order to quantify deviations, as expressed in Equation (3).

$$D_i = |H_{ATL03} - H_{SYM12}| \tag{3}$$

To identify and eliminate outliers within the set of absolute elevation differences, the Interquartile Range (IQR) method was employed (Yuan et al., 2020; Kaya et al., 2023). The IQR was computed using Equations (4), (5), and (6).

$$IQR = Q_3 - Q_1 \tag{4}$$

$$Lower\ bound = Q_1 - 1.5 \times IQR \tag{5}$$

$$Upper\ bound = Q_3 + 1.5 \times IQR \tag{6}$$

where, Q_1 and Q_3 represent the first and third quartiles, respectively. Outliers among the elevation differences between each ATL03 photon and SYM12 grid cell were identified as those values falling below the lower threshold or above the upper threshold, and were subsequently excluded from the dataset.

2.3.4. Download and preprocessing of AT03 data

In this study, the performance of the ICESat-2 ATL03 and SYM12 datasets was evaluated in terms of vertical agreement and overall accuracy. The analysis was conducted in two main stages. In the first stage, the consistency of elevation values between ATL03 and SYM12 was examined to determine the degree of alignment between the two datasets. In the second stage, the reliability of each dataset was assessed by comparing their elevation values against orthometric heights derived from GPS measurements. For this purpose, the evaluation of model performance was carried out using Root Mean Square Error (RMSE), Mean Absolute Error (MAE), and the Pearson correlation coefficient (R).

RMSE (Root Mean Square Error) measures the overall magnitude of differences between the predicted elevation values and the reference elevation values. MAE (Mean Absolute Error), on the other hand, represents the average of the absolute values of these errors and is less sensitive to extreme outliers compared to RMSE. RMSE and MAE are calculated according to Equations (7) and (8), respectively.

$$RMSE = \sqrt{\frac{1}{n} \sum_{i=1}^n (H_{model,i} - H_{ref,i})^2} \tag{7}$$

$$MAE = \frac{1}{n} \sum_{i=1}^n |H_{model,i} - H_{ref,i}| \tag{8}$$

where, $H_{model,i}$ represents the elevation value obtained from ATL03 or SYM12, $H_{ref,i}$ denotes the reference elevation derived from GPS, and n is the number of points used in the comparison.

The Pearson correlation coefficient (R) quantitatively describes the linear relationship between two elevation datasets. In this study, the correlation was first calculated between ATL03 and SYM12, and then between GPS and each of ATL03 and SYM12. The R coefficient is calculated using Equation (9).

$$= \frac{\sum_{i=1}^n (H_{model,i} - \bar{H}_{model})(H_{ref,i} - \bar{H}_{ref})}{\sqrt{\sum_{i=1}^n (H_{model,i} - \bar{H}_{model})^2} \sqrt{\sum_{i=1}^n (H_{ref,i} - \bar{H}_{ref})^2}} \tag{9}$$

where \bar{H}_{model} ve \bar{H}_{ref} represent the mean model elevation and mean reference elevation, respectively.

The Pearson correlation coefficient ranges between -1 and 1. Values close to 1 indicate a strong positive correlation, while values close to -1 indicate a strong negative correlation. As the correlation coefficient approaches zero, the relationship between the two datasets becomes weaker, indicating little to no correlation.

3. Results

3.1. Comparison of SYM12 and ATL03 elevations

The comparative analysis of SYM12 and ATL03_{TG20} elevation datasets highlights the agreements and discrepancies within the study area. Figure 3 presents scatter plots of SYM12 and ATL03-TG20 elevation values for both unfiltered and filtered datasets, illustrating the distribution and relationship of the elevation measurements.

The Pearson correlation coefficient ranges between -1 and 1. Values close to 1 indicate a strong positive

Comparison of SYM12 and ATL03_{TG20} Elevations

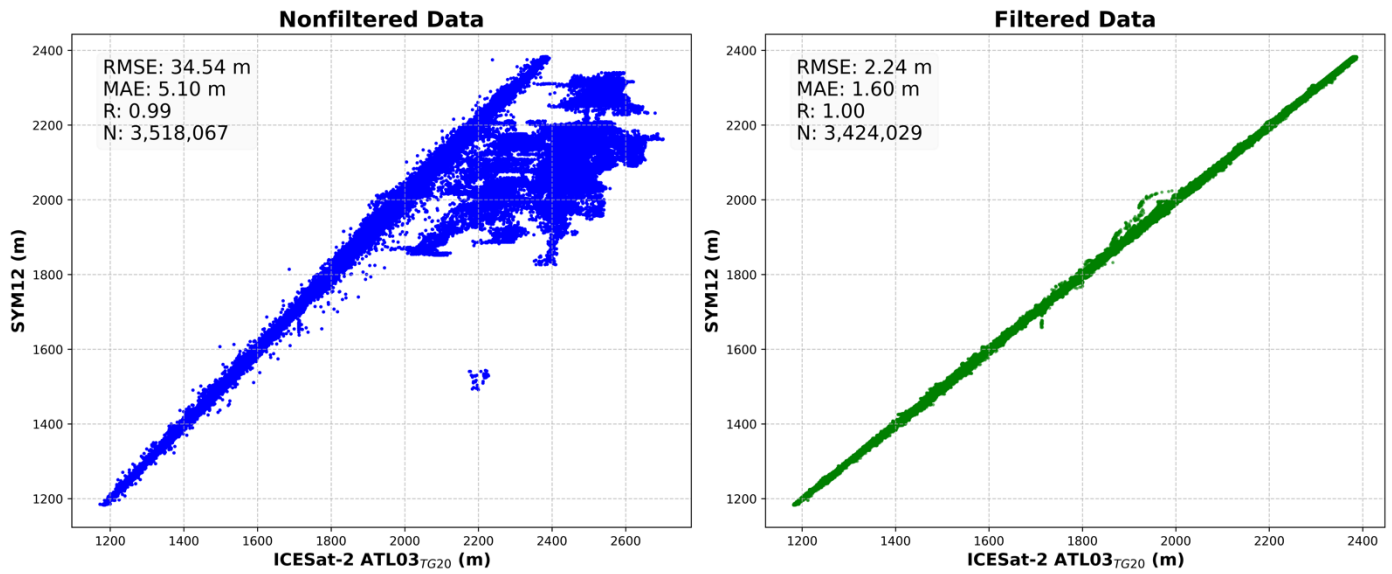


Figure 3. Comparison of SYM12 and ATL03-TG20 Elevations

As shown in Figure 3, the unfiltered dataset exhibits a highly scattered distribution. This dispersion is primarily associated with the presence of outlier points, which reflect significantly large vertical discrepancies. These outliers may result from inconsistencies in terrain surface modeling, measurement or sensor errors, or other systematic and random errors introduced during data processing. Such discrepancies can also be attributed to the limitations of radar interferometry and the 12-meter resolution of the SYM12 model, which may not perfectly align with the ATL03-TG20 data. Factors such as radar interaction with vegetation and radar shadowing in complex topography are known constraints of interferometric methods that may lead to mismatches with photon-counting LiDAR data. The Root Mean Square Error (RMSE) and Mean Absolute Error (MAE) calculated for the unfiltered dataset 34.54 m and 5.10 m, respectively demonstrate the significant influence of outliers on the overall error statistics.

In contrast, the filtered dataset shows a much tighter clustering of points around the 1:1 line, indicating a stronger agreement between the two datasets after the removal of outliers. The elimination of extreme values more clearly reveals the true correlation between SYM12 and ATL03-TG20. As a result of the filtering process, the RMSE and MAE were significantly reduced to 2.24 m and 1.60 m, respectively. This notable improvement demonstrates that the IQR-based outlier elimination method effectively identified extreme values and enhanced the overall data integrity. These findings suggest that SYM12 and ATL03-TG20 are in fact highly correlated, but that a small number of outliers had previously distorted this relationship. Nonetheless, the presence of minor differences in the filtered dataset may still be attributed to several factors, such as terrain complexity, limitations inherent in the radar data used to generate SYM12 (e.g., interactions with vegetation or man-made structures), errors introduced during the TG20 geoid transformation, or differences in spatial resolution between the datasets. To further investigate these discrepancies, Figure 4 presents histograms of RMSE and MAE distributions for both the raw and filtered datasets. These visualizations facilitate a clearer understanding of the range and frequency of errors by showing where error values are concentrated and where they occur less frequently.

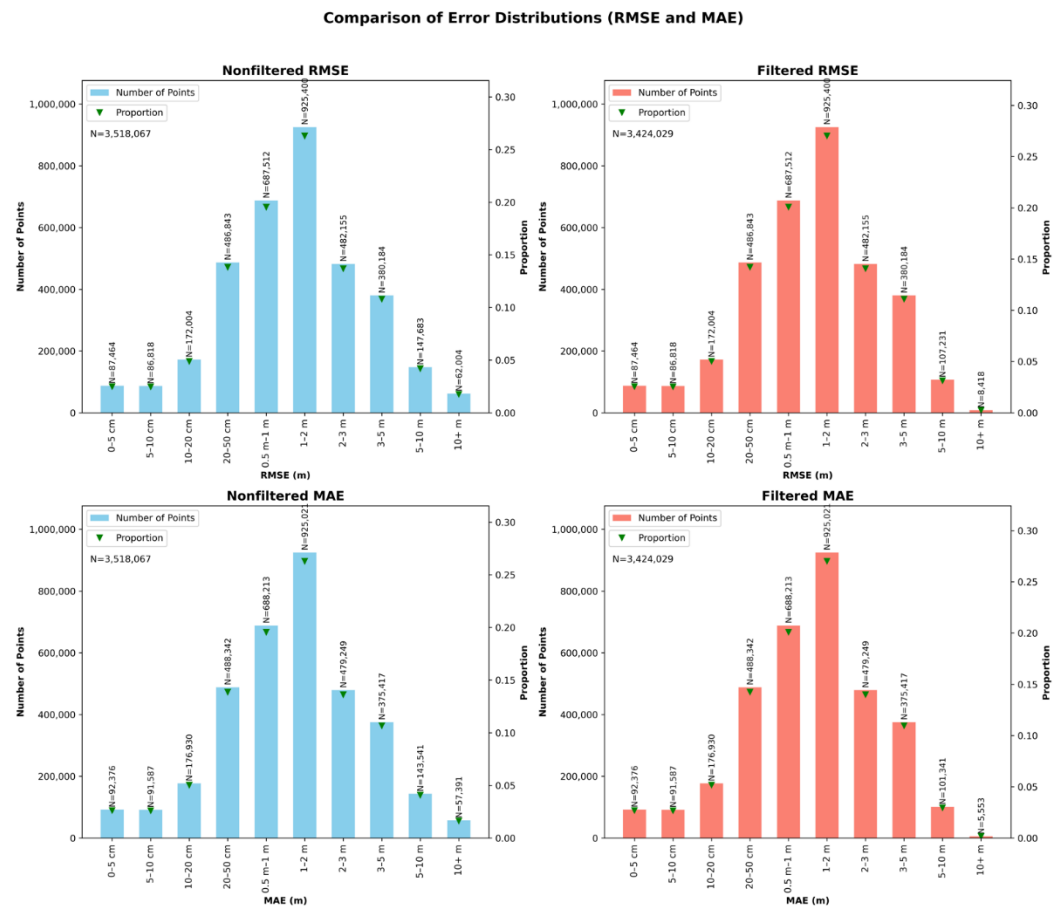


Figure 4. Comparison of RMSE and MAE Error Distributions

An examination of the unfiltered data in Figure 4 reveals a wide distribution of RMSE and MAE values, confirming the presence of numerous extreme discrepancies within the dataset. In particular, the high concentration of error values exceeding 10 meters negatively influences the overall error metrics. Similarly, the MAE distribution indicates a substantial proportion of points with large deviations, further supporting this observation. In contrast, the histograms of the filtered dataset show that both RMSE and MAE values are tightly clustered within a narrow range. This indicates a more consistent error distribution, with the majority of values falling below 2–3 meters after outlier removal. The high frequency of MAE values in the 1–2-meter range suggests that the SYM12 model generally aligns well with ATL03-TG20 data. Nevertheless, a closer look at the histograms reveals that, although relatively few in number, there are still some points with RMSE and MAE values in the 5–10 meter and >10-meter ranges. These points highlight areas where the model may underperform, particularly in regions with complex topography or dense vegetation cover. This is consistent with observations from Figure 3, where larger errors were clearly visible in mountainous regions with steep slopes. To provide further insight into the spatial distribution and impact of these elevation differences on error metrics, Figure 5 presents a detailed analysis of RMSE and MAE values across the study area.

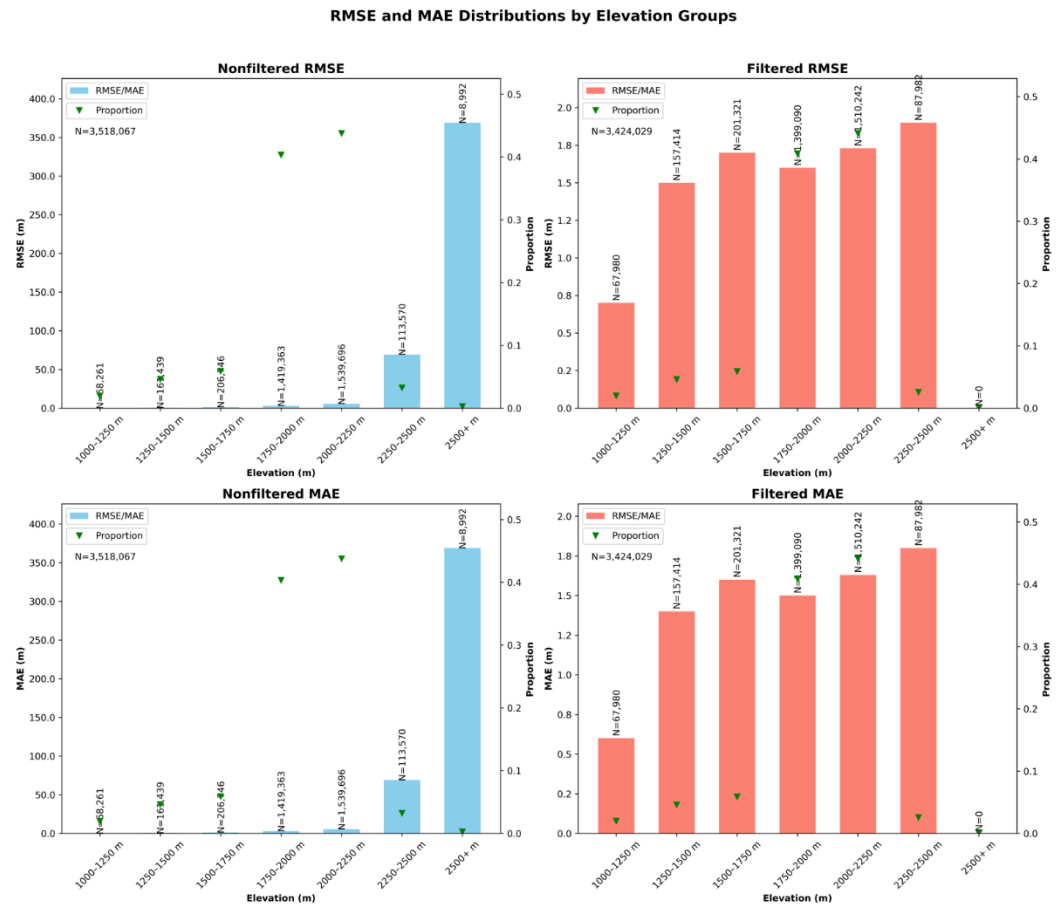


Figure 5. Comparison of RMSE and MAE Distributions by Elevation Groups

As illustrated in Figure 5, the influence of elevation on RMSE and MAE values is clearly evident. In relatively low-altitude areas (e.g., 0–500 m), there is a stronger agreement between SYM12 and ATL03_{TG20}, as indicated by notably low RMSE and MAE values. This improved performance can be attributed to the more homogeneous surface characteristics typically found in low-slope or urbanized regions, where phase ambiguities during radar processing are less likely due to gentler terrain. Additionally, geoid transformations within this elevation range tend to yield less complex results. Conversely, in mountainous and rugged areas above 1500 meters, a substantial increase in both RMSE and MAE values is observed. The steep slopes and rapidly varying topographic transitions in these high-altitude zones may include terrain details too fine to be accurately captured by the 12-meter resolution of the SYM12 model. Radar interferometry also struggles to maintain phase coherence in regions with steep inclines or dense forest cover. Furthermore, regional variations in geoid surfaces may become more pronounced at higher elevations, potentially introducing additional vertical error during the conversion to orthometric heights using the TG20 model. In conclusion, the combination of these factors contributes to a decrease in SYM12 performance in higher elevation zones. Even after outlier filtering, this trend is not entirely eliminated, suggesting persistent challenges in accurately modeling elevation under such complex terrain conditions.

In summary, the combined evaluation of Figures 3, 4, and 5 reveals a generally high level of consistency between SYM12 and ATL03_{TG20}, though this consistency varies depending on whether the dataset has been filtered and the topographic characteristics of the terrain. After filtering, SYM12 demonstrates strong accuracy in low- to mid-elevation areas, typically within the 2–3 meter range. However, at higher elevations, error values tend to increase. The substantial reduction in total error following outlier removal suggests that many of the extreme discrepancies are likely due to localized issues in measurement or data acquisition,

rather than systematic flaws in the model itself. This supports the notion that the core structure of the SYM12 model is fundamentally sound, and that the majority of large errors are not inherently systematic.

In conclusion, SYM12 demonstrates strong potential as a reliable elevation dataset for general use, particularly in flat or gently sloping terrain, where its performance is found to be satisfactory. However, when applied in highly mountainous or topographically complex regions, it is recommended that analyses based on SYM12 be supported with in-situ validation or additional remote sensing techniques. This study reaffirms the potential of high-accuracy ATL03_{TG20} photon data for the validation and enhancement of radar-based digital surface models, such as SYM12. The statistical results and visual analyses derived from varying terrain conditions clearly highlight both the strengths and limitations of SYM12. The findings indicate that while SYM12 can already provide valuable contributions to disciplines such as geosciences, disaster management, urban planning, and engineering, further validation and correction steps may be required in complex terrains. This comprehensive evaluation contributes to a better understanding of the factors influencing vertical consistency between SYM12 and ATL03_{TG20} datasets. Accordingly, future studies aiming to minimize model-data discrepancies may consider incorporating robust outlier removal procedures and terrain-specific model enhancement techniques tailored for complex landscapes.

3.2. Validation of SYM12 and ATL03-TG20 Data Using Ground Observations

The ground-based evaluation was conducted to assess the extent to which the SYM12 and ATL03_{TG20} datasets accurately represent the current surface conditions. For this purpose, a network of 879 control points obtained via GPS measurements was used, strategically selected to cover a variety of land surface types and elevation ranges. The GPS-derived elevations were converted to orthometric heights using the TG20 geoid model. These GPS-TG20 elevations were then compared against both the SYM12 and ATL03_{TG20} datasets to evaluate their respective accuracies (Figure 6).

Comparison of SYM12 and ATL03_{TG20} Values with GPS_{TG20}

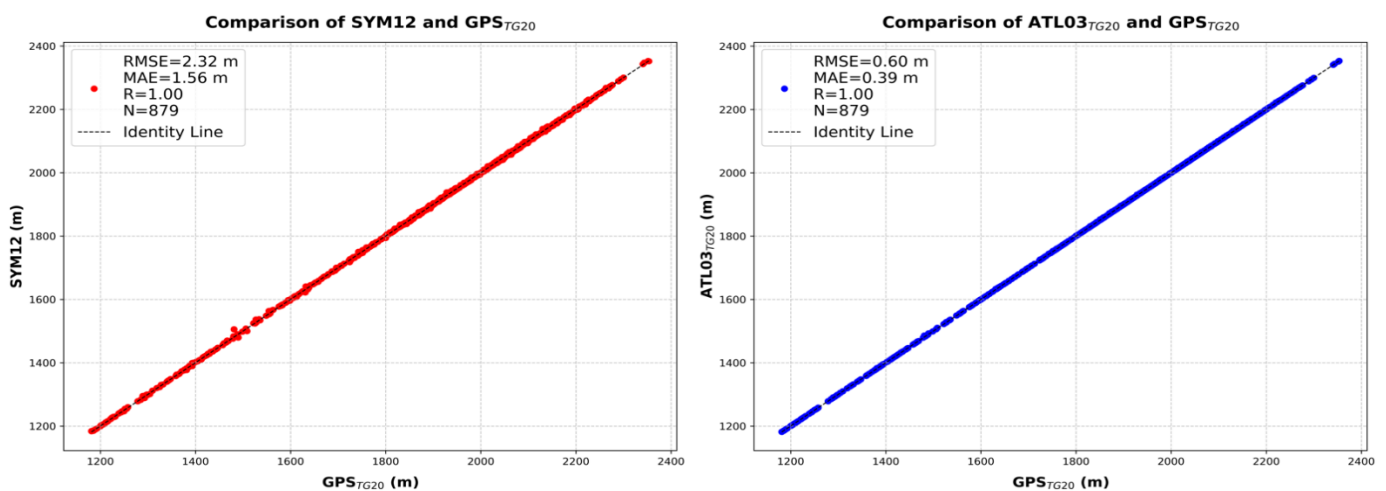


Figure 6. Comparison of SYM12 and ATL03_{TG20} Data with GPS-TG20 Elevations

The results presented in Figure 6 indicate that both datasets exhibit a high level of correlation with the GPS reference data, with $R > 0.99$. The scatter plots show that point clouds from both SYM12 and ATL03_{TG20} are tightly clustered around the 1:1 line, suggesting that both datasets generally reflect regional elevation variations accurately. However, when examining RMSE and MAE values, which directly reflect the magnitude of error, it becomes evident that ATL03_{TG20} aligns more closely with ground observations. The RMSE and MAE

for SYM12 relative to GPS data were calculated as 2.32 m and 1.56 m, respectively, whereas for ATL03_{TG20}, these metrics dropped significantly to 0.60 m and 0.39 m. One of the main reasons behind this difference lies in the temporal range of data acquisition. SYM12 is based on radar interferometry data collected between 2011 and 2014, while ATL03_{TG20} is derived from more recent ICESat-2 photon data (2018–2023). Furthermore, the GPS observations used in this study were collected in 2024, which may have amplified the temporal aging effect of the SYM12 dataset. Natural surface changes over time such as erosion, deposition, construction activities, or vegetation growth may have caused SYM12 to lag behind the actual surface conditions. Another significant factor is the type of remote sensing technology employed. Radar interferometry tends to capture reflections from canopy tops or other elevated surfaces in vegetated or uneven areas, potentially overestimating terrain elevation. In contrast, ATL03_{TG20}, based on photon-counting laser altimetry, has a greater capacity to penetrate vegetation and provide more accurate measurements of ground-level elevation. Additionally, the 12-meter gridded resolution of SYM12 may limit its ability to represent fine-scale topographic details, particularly in microtopographically complex regions. ATL03-TG20, on the other hand, offers sub-meter point-based precision, allowing for a much closer alignment with GPS-TG20 observations. This difference is also visually supported by the scatter plots in Figure 6, where the spread of SYM12 points around the 1:1 line appears slightly wider than that of ATL03_{TG20}. This pattern statistically confirms that SYM12 exhibits greater deviations in areas with high surface roughness or rapidly changing terrain features.

Considering temporal land surface changes and the differences in sensing technologies, it becomes increasingly expected that ATL03-TG20 yields results more closely aligned with GPS observations compared to SYM12. Therefore, while SYM12 remains a valuable resource for large-scale analyses and macro-scale topographic assessments, ATL03-TG20 emerges as the superior choice for applications requiring high accuracy or aiming to monitor recent surface changes. Moreover, the integration of SYM12 and ATL03-TG20 datasets holds the potential to produce hybrid elevation models that combine broad spatial coverage with fine-scale accuracy. Such an approach could offer more functional solutions for applications in terrain change analysis, disaster management, engineering projects, and spatial planning. These findings highlight the importance of selecting datasets based on the specific goals of a study, the required spatial resolution, and the temporal currency of the data. As also shown in Figure 6, the extremely high correlation between both datasets and GPS measurements confirms the scientific and practical value of both SYM12 and ATL03_{TG20}. However, the lower RMSE and MAE values observed between ATL03-TG20 and GPS underscore the necessity of using laser-based datasets when seeking the most accurate and up-to-date representation of terrain surfaces. Finally, it is important to emphasize that the discrepancy between SYM12 and GPS measurements may also be influenced by the temporal gap between data acquisitions. SYM12 was generated from radar data collected between 2011 and 2014, whereas the GPS dataset used in this study reflects the surface condition as of 2024. This significant time difference could have led to changes in terrain due to erosion, land use transformation, vegetation dynamics, or construction activities, which are not captured in the SYM12 model. Therefore, this temporal mismatch is acknowledged as a key limitation of the analysis.

4. Discussion and Conclusions

The comparative evaluation of SYM12, ICESat-2 ATL03, and ground-based GPS observations underscores the interplay between data acquisition periods, sensor technologies, and topographic complexity in determining vertical accuracy. While SYM12 effectively characterizes broad-scale elevation patterns in low- and mid-altitude regions, its performance deteriorates in high-altitude, rugged, or densely vegetated areas. This trend reflects the well-known limitations of radar interferometry, particularly its susceptibility to phase decorrelation and signal penetration issues under complex surface conditions. The

temporal mismatch between SYM12 acquisitions (2011–2014), ATL03 data (2018–2023), and GPS measurements (2024) further exacerbates observed discrepancies by highlighting land surface changes that have occurred in the intervening years. In contrast, ATL03 benefits from photon-counting LiDAR technology, more recent data acquisition, sub-meter spatial precision, and the ability to accurately detect ground surfaces beneath vegetation canopies. As a result, ATL03 consistently achieves lower RMSE and MAE values relative to GPS references, demonstrating its high potential as a source of high-resolution and high-accuracy DSMs. These attributes make ATL03 particularly well-suited for fine-scale applications such as infrastructure design, flood risk assessment, and precision agriculture. Furthermore, the comparison between SYM12 and the GPS dataset collected in 2024, which yielded higher RMSE (2.32 m) and MAE (1.56 m) values relative to ATL03 (RMSE = 0.60 m; MAE = 0.39 m), indicates a temporal aging effect associated with SYM12. Since SYM12 was derived from data acquired between 2011 and 2014, it may no longer accurately represent current surface conditions due to natural and anthropogenic changes over the past decade. This emphasizes the importance of dataset currency in DSM accuracy assessments and highlights the need for regular updates or hybridization with more recent datasets like ICESat-2 ATL03 to mitigate time-induced discrepancies.

Despite its limitations, SYM12 remains a valuable resource due to its broad spatial coverage and relatively fine resolution for a nationally produced, radar-based DSM. In less dynamic or topographically simpler landscapes, SYM12 continues to provide sufficiently accurate elevation information. Therefore, the integration of SYM12 and ATL03 offers a promising pathway toward the development of hybrid DSM products that leverage the extensive coverage of SYM12 and the temporal continuity and technological advantages of ATL03. Such integration could significantly enhance vertical accuracy across large areas—particularly if an optimal calibration or fusion strategy is developed to reconcile the error characteristics of both datasets. The findings of this study carry important implications for practical applications. In particular, high-accuracy elevation datasets are essential for infrastructure planning, precision mapping, and natural disaster management. The demonstrated superiority of ICESat-2 ATL03 over older radar-derived DSMs highlights the need to adopt more recent and sensitive data sources in these contexts. Furthermore, the integration of datasets such as ATL03 and SYM12 could facilitate cost-effective solutions in large-area modeling while retaining high spatial accuracy in critical zones.

Looking ahead, several research directions emerge. First, addressing the temporal gaps in radar-derived DSMs is essential; regularly or more frequently updating SYM12 could reduce inconsistencies caused by land cover changes, erosion, or anthropogenic activities. Second, the application of advanced machine learning and data fusion techniques may enhance the integration of SYM12 and ATL03 by systematically identifying and correcting regional biases or localized anomalies. Third, the development of region-specific calibration approaches that account for local factors such as slope, vegetation type, or geological characteristics could further improve the accuracy of radar-based models. Finally, the inclusion of additional datasets—such as UAV-based photogrammetry or terrestrial LiDAR—could strengthen validation frameworks and support the generation of more reliable, multi-scale DSMs.

In conclusion, this study demonstrates that radar-based DSMs such as SYM12 can benefit significantly from the integration of more recent and precise LiDAR datasets like ICESat-2 ATL03. Such multi-source strategies are increasingly important in addressing the demand for higher accuracy and up-to-date spatial information, particularly in rapidly changing landscapes. Future research can further enhance the scientific and practical value of these datasets for monitoring, planning, and managing the Earth's dynamic surface by focusing on systematic DSM updates, the adoption of state-of-the-art fusion techniques, and the calibration of models to region-specific conditions.

Acknowledgments: I would like to express my gratitude to the General Directorate of Mapping (HGM) for providing the SYM12 and TG20 datasets, and to the National Snow and Ice Data Center (NSIDC) for access to the ICESat-2 ATL03 data.

Author Contributions: A single author carried out the study.

Research and publication ethics statement: In the study, the author declares that there is no violation of research and publication ethics and that the study does not require ethics committee approval.

Conflicts of Interest: The author declares no conflicts of interest.

References

- Anders, N., Smith, M., Suomalainen, J., Cammeraat, E., Valente, J., & Keesstra, S. (2020). Impact of flight altitude and cover orientation on digital surface model (DSM) accuracy for flood damage assessment in Murcia (Spain) using a fixed-wing UAV. *Earth Science Informatics*, 13, 391–404. <https://doi.org/10.1007/s12145-019-00427-7>
- Courellis, H. S., Iversen, J. R., Poizner, H., & Cauwenberghs, G. (2016). EEG channel interpolation using ellipsoid geodesic length. *Proceedings Book of IEEE Biomedical Circuits and Systems Conference (BioCAS)*, Shanghai, China. 540–543.
- Dibs, H., Al-Ansari, N., & Laue, J. (2023). Analysis of remotely sensed imagery and architecture environment for modelling 3D detailed buildings using geospatial techniques. *Engineering*, 15(5), 328–341. <https://doi.org/10.4236/eng.2023.155026>
- Gao, M., Xing, S., Zhang, G., Zhang, X., & Li, P. (2023). Assessment of ICESat-2's horizontal accuracy using an iterative matching method based on high-accuracy terrains. *Remote Sensing*, 15(9), 2236. <https://doi.org/10.3390/rs15092236>
- Gazioğlu, C., Aipar, B., Yücel, Z. Y., Müftüoğlu, A. E., Güneysu, C., Ertek, T. A., Demir, V., & Kaya, H. (2014). Morphologic features of Kapıdağ Peninsula and its coasts (NW-Turkey) using by remote sensing and DTM. *International Journal of Environment and Geoinformatics*, 1(1), 48–63. <https://doi.org/10.30897/ijgeo.300739>
- Guo, K., Guan, M., & Yu, D. (2021). Urban surface water flood modelling—A comprehensive review of current models and future challenges. *Hydrology and Earth System Sciences*, 25(5), 2843–2860. <https://doi.org/10.5194/hess-25-2843-2021>
- Joshi, N., Baumann, M., Ehammer, A., Fensholt, R., Grogan, K., Hostert, P., Jepsen, M. R., Kuemmerle, T., Meyfroidt, P., Mitchard, E. T. A., Reiche, J., Ryan, C. M., & Waske, B. (2016). A review of the application of optical and radar remote sensing data fusion to land use mapping and monitoring. *Remote Sensing*, 8(1), 70. <https://doi.org/10.3390/rs8010070>
- Karataş, H., & Yaman, A. (2024). Investigation of the usability of Göktürk-2 data and UAV data for pond construction project. *The Egyptian Journal of Remote Sensing and Space Sciences*, 27(3), 565–576. <https://doi.org/10.1016/j.ejrs.2024.07.002>
- Kaya, Y., Sanli, F. B., & Abdikan, S. (2023). Determination of long-term volume change in lakes by integration of UAV and satellite data: The case of Lake Burdur in Türkiye. *Environmental Science and Pollution Research*, 30(55), 117729–117747. <https://doi.org/10.1007/s11356-023-30369-z>
- Kılıç, B., Gülgen, F., Çelen, M., Öncel, S., Oruç, H., & Vural, S. (2022). Morphometric analysis of Saz-Çayırova drainage basin using geographic information systems and different digital elevation models. *International Journal of Environment and Geoinformatics*, 9(2), 177–186. <https://doi.org/10.30897/ijgeo.1079851>
- Li, B., Xie, H., Liu, S., Ye, Z., Hong, Z., Weng, Q., Sun, Y., Xu, Q., & Tong, X. (2024). Global DEM product generation by correcting ASTER GDEM elevation with ICESat-2 altimeter data. *Earth System Science Data Discussions*, 2024, 1–24. <https://doi.org/10.5194/essd-17-205-2025>
- Li, B., Xie, H., Tong, X., Tang, H., & Liu, S. (2023). A global-scale DEM elevation correction model using ICESat-2 laser altimetry data. *IEEE Transactions on Geoscience and Remote Sensing*, 61, 1-15. <https://doi.org/10.1109/TGRS.2023.3321956>
- Li, H., Zhao, J., Yan, B., Yue, L., & Wang, L. (2022a). Global DEMs vary from one to another: An evaluation of newly released Copernicus, NASA and AW3D30 DEM on selected terrains of China using ICESat-2 altimetry data. *International Journal of Digital Earth*, 15(1), 1149–1168. <https://doi.org/10.1080/17538947.2022.2094002>
- Li, Y., Fu, H., Zhu, J., Wu, K., Yang, P., Wang, L., & Gao, S. (2022b). A method for SRTM DEM elevation error correction in forested areas using ICESat-2 data and vegetation classification data. *Remote Sensing*, 14(14), 3380. <https://doi.org/10.3390/rs14143380>
- Loew, A., Bell, W., Brocca, L., Bulgin, C. E., Burdanowitz, J., Calbet, X., Donner, R. V., Ghent, D., Gruber, A., Kaminski, T., Kinzel, J., Klepp, C., Lambert, J. C., Schaepman-Strub, G., Schröder, M., & Verhoelst, T. (2017). Validation practices for satellite-based Earth observation data across communities. *Reviews of Geophysics*, 55(3), 779–817. <https://doi.org/10.1002/2017RG000562>
- Mesa-Mingorance, J. L., & Ariza-López, F. J. (2020). Accuracy assessment of digital elevation models (DEMs): A critical review of practices of the past three decades. *Remote Sensing*, 12(16), 2630. <https://doi.org/10.3390/rs12162630>
- Moore, I. D., Turner, A. K., Wilson, J. P., Jenson, S. K., & Band, L. E. (1993). GIS and land-surface-subsurface process modeling. Environmental Modeling with GIS, Oxford University Press, Inc.
- Neumann, T. A., Brenner, A., Hancock, D., Robbins, J., Saba, J., Harbeck, K., ... & Rebold, T. (2020). ATLAS/ICESat-2 L2A global geolocated photon data, version 3. NASA National Snow and Ice Data Center Distributed Active Archive Center, Boulder, CO, United States.

- Oksanen, J., & Sarjakoski, T. (2005). Error propagation of DEM-based surface derivatives. *Computers & Geosciences*, 31(8), 1015–1027. <https://doi.org/10.1016/j.cageo.2005.02.014>
- Panda, S. S., Rao, M. N., Thenkabail, P. S., Misra, D., & Fitzgerald, J. P. (2016). Remote sensing systems—platforms and sensors: Aerial, satellite, UAV, optical, radar, and LiDAR. *Remote Sensing Handbook*. CRC Press.
- Quamar, M. M., Al-Ramadan, B., Khan, K., Shafiullah, M., & El Ferik, S. (2023). Advancements and applications of drone-integrated geographic information system technology—A review. *Remote Sensing*, 15(20), 5039. <https://doi.org/10.3390/rs15205039>
- Rosen, P. A., Hensley, S., Joughin, I. R., Li, F. K., Madsen, S. N., Rodriguez, E., & Goldstein, R. M. (2000). Synthetic aperture radar interferometry. *Proceedings of the IEEE*, 88(3), 333–382. <https://doi.org/10.1109/5.838084>
- Sahani, J., Kumar, P., Debele, S., Spyrou, C., Loupis, M., Aragão, L., Feredico, P., Shah, M. A. R., & Di Sabatino, S. (2019). Hydro-meteorological risk assessment methods and management by nature-based solutions. *Science of the Total Environment*, 696, 133936. <https://doi.org/10.1016/j.scitotenv.2019.133936>
- Schumann, G. J. P., Muhlhausen, J., & Andreadis, K. M. (2019). Rapid mapping of small-scale river-floodplain environments using UAV SfM supports classical theory. *Remote Sensing*, 11(8), 982. <https://doi.org/10.3390/rs11080982>
- Schutz, B. E., Zwally, H. J., Shuman, C. A., Hancock, D., & DiMarzio, J. P. (2005). Overview of the ICESat mission. *Geophysical Research Letters*, 32(21). <https://doi.org/10.1029/2005GL024009>
- Shen, X., Ke, C. Q., Fan, Y., & Drolma, L. (2022). A new digital elevation model (DEM) dataset of the entire Antarctic continent derived from ICESat-2. *Earth System Science Data*, 14(7), 3075–3089. <https://doi.org/10.5194/essd-14-3075-2022>
- Simav, M., Akpınar, İ., Akdoğan, Y. A., & Yıldız, H. (2021). Recent terrestrial gravimetry studies in Turkey. *Harita Dergisi*, 166(July), 10–24.
- Ulvi, A., & Yiğit, A. Y. (2022). Comparison of the wearable mobile laser scanner (WMLS) with other point cloud data collection methods in cultural heritage: A case study of Diokaisareia. *ACM Journal on Computing and Cultural Heritage*, 15(4), 1–19. <https://doi.org/10.1145/3551644>
- Van Westen, C. J. (2013). Remote sensing and GIS for natural hazards assessment and disaster risk management. *Treatise on Geomorphology*, 3(15), 259–298.
- Yiğit, A. Y., Hamal, S. N. G., Yakar, M., & Ulvi, A. (2023). Investigation and implementation of new technology wearable mobile laser scanning (WMLS) in transition to an intelligent geospatial cadastral information system. *Sustainability*, 15(9), 7159. <https://doi.org/10.3390/su15097159>
- Yıldız, H., Simav, M., Sezen, E., Akpınar, İ., Akdoğan, Y. A., Cingöz, A., & Akabali, O. A. (2021). Determination and validation of the Turkish Geoid Model-2020 (TG-20). *Bulletin of geophysics and oceanography*, 62, 495–512.
- Yuan, C., Gong, P., & Bai, Y. (2020). Performance assessment of ICESat-2 laser altimeter data for water-level measurement over lakes and reservoirs in China. *Remote Sensing*, 12(5), 770. <https://doi.org/10.3390/rs12050770>